Study of filament dynamics using synthetic and experimental BES diagnostics

O. Asztalos[1,2], A.H. Nielsen[3], I. Andorfi[1], D. Dunai[2], S. Zoletnik[2], D.I. Refy[2], B. Tál[4], G. Birkenmeier[4], R. Coelho[5], G.I. Pokol[1,2], EU-IM Team[*], EUROfusion-MST1 Team[**], ASDEX Upgrade Team[***]

[1] *Institute for Nuclear Techniques, BME, 1111 Műegyetem rakpart 9-11, Budapest, Hungary*
[2] *Centre for Energy Research, Budapest, Hungary*
[3] *Plasma Physics and Fusion Energy, Department of Physics, DTU, 2800 Kgs. Lyngby, Denmark*
[4] *Max-Planck Institute for Plasma Physics, Boltzmannstrasse 2, 85748 Garching, Germany*
[5] *IPNF, IST, Universidade de Lisboa, Av. Rovisco Pais 1, 1049-001 Lisboa, Portugal*
[*] *https://users.euro-fusion.org/eu-im*
[**] *See author list at Labit B. et al., Nucl. Fusion 59 086020 (2019)*
[***] *See the author list of H. Meyer et al. Nucl. Fusion 59 112014 (2019)*

Introduction The scrape-off layer (SOL) is located on the outside of the confined plasma region of fusion devices and serves as a boundary condition for plasma confinement as well as an exhaust for particles and energy. Understanding the physics and behaviour of the SOL is paramount to manage heat loads on plasma facing components or improve overall plasma performance. SOL turbulence and subsequently emergent filament dynamics play a defining role in SOL physics [1]. To this end, a turbulence workflow was developed and used within the EU-IM framework [2] in an effort to compare experimental measurements of SOL turbulence, with synthetic ones derived from first principle plasma physics codes.

The turbulence workflow uses HESEL [3], a 2D, multi-field, drift-fluid code to generate turbulence data, initialized using plasma profiles derived from experimental measurements. The turbulence workflow was coupled to a beam emission spectroscopy (BES) workflow using the RENATE [4] fully 3D BES modelling code to generate synthetic measurement signals. A model validation effort was carried out using BES measurements on the L-mode part of ASDEX-Upgrade discharge #29302 [5], as a well-established reference.

BES synthetic diagnostic Previous work concerning the application of synthetic BES diagnostics was published in Nielsen et al. [6] showing a systematic discrepancy in the comparison of experimental and corresponding synthetic signals. In order to overcome such discrepancies, a concise definition for what constitutes a synthetic diagnostic was put forward: "*Any diagnostics model functions as a synthetic diagnostic, if all relevant diagnostic artefacts affecting signal properties, characteristic to a well specified measurement task, are accounted for"*. Relevant BES diagnostics artefacts for synthetic plasma turbulence measurements are the ones affecting the filament perception throughout the detection process.

- Direct collisional radiative model solver: Deals with correct beam atom valence electron distribution calculation on excited states over plasma density gradients [4].
- Spatial smoothing of beam emission: Deals with the emission smearing specific to BES from the alignment of the magnetic and observation geometries and atomic physics processes [7].
- Noise modelling: Deals with the signal transformation from the deterministic, expected BES photon current values to noisy, BES specific, signal voltage values.

Noise models The ASDEX-Upgrade LiBES system is equipped with Hamamatsu R928 Photomultiplier Tubes (PMT), featuring a quantum efficiency (Q_E) 0.07 @ 670 nm; dynode gain (δ) 6; dynode number (n) 9; bandwidth (B) 100 kHz; dark current (I_D) 25 nA and load resistance (R_L) [8]. Relevant noise sources characteristic to PMT detectors are the shot, dark and Johnson noise terms, which are applied to the total expected photon current (Φ_T) on each detector. The total expected photon current consisting of background emission added to the expected photon current derived by RENATE. Two noise models were derived:

a) Gaussian model was developed based on previous work done by Dunai *et al.*[9], relying on the superposition of Gaussian distributions for each noise term, described by following equation: $S_G(t) = R_L\left[N_{shot}\left(U_s(t), \sigma_s(t)\right) + N_{dark}(U_d, \sigma_d)\right] + N_J\left(U_J, \sigma_J\right)$,where the shot noise ($N_{shot}$), dark noise ($N_{dark}$) and Johnson noise ($N_J$) are defined by their respective mean values $(2eB\delta^n Q_E \Phi_T(t);\ I_D;\ 0)$ as well as their respective variances $\left(\sqrt{2eB\delta^n \frac{\delta}{\delta-1} U_s(t)};\ \sqrt{4eB\delta^n \frac{\delta}{\delta-1} U_d};\ \sqrt{4k_B T B R_L}\right)$.

b) Detailed model statistically follows the electron generation through the photon detection process. Electron generation and gain on PMTs various components follow Poisson distributions. The final noisy synthetic signal is given by: $S_D(t) = 2eBR_L \times Pois\left(n_{sn}(t)\right) + N_J\left(U_J, \sigma_J\right)$, where the second term describes the Johnson noise. The first term recursively describes secondary electron generation through the PMT, $n_{sx}(t) = Pois\left(n_{s(x-1)}(t)\delta\right)$, where $n_{s0}(t) = n_c(t)$ gives the initial cathode emitted electrons. The cathode electron generation follows $n_c(t) = Pois\left[Pois\left(\frac{\Phi_T}{2B}\right) Q_E\right] + D\left(\frac{I_D}{2eB\delta^n}\right)$, where the first term describes the photon induced electron fraction, while the second term the dark electron generation.

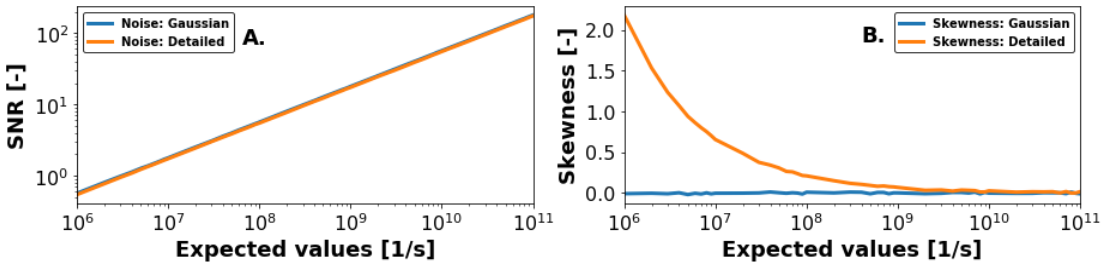

Figure 1: Comparison of Gaussian and Detailed noise models for constant expected value time series. A: shows SNR comparison. B: shows skewness comparison.

A comparison of the two different noise models showed identical signal to noise values for a wide range of constant value expected time signals (Figure 1A.), while higher signal moments, such as the skewness (Figure 1B.) revealed diverging behaviour, inferring both models generating signal to noise values in accordance with manufacturer specifications, while the detailed noise models sensitivity for triggering counts at low photon levels make it preferable for ASDEX-Upgrade. Figure 2 A. and B. show the skewness and kurtosis for the same synthetic BES signal scaled for various expected mean signal values. As high photon counts supress the noise, both models converge to the expected signal skewness and kurtosis and later start diverging from it, as the mean expected photon count drops. The models diverge in skewness and kurtosis in the range of 10^7 – 10^8 1/s.

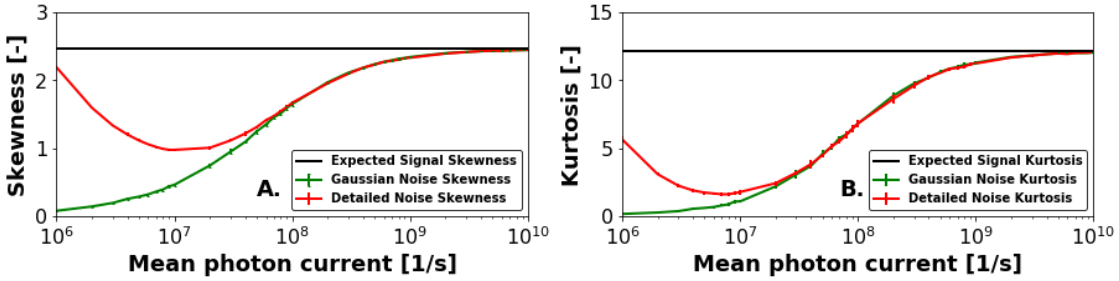

Figure 2: Shows the skewness (A.) and kurtosis (B.) of the same synthetic BES signal scaled for different mean expected signal values.

Validation A qualitative validation attempt was made by assessing the skewness (S) and kurtosis (K) of time signals corresponding to the same observation channels. The S and K of the HESEL density time signal (red), the expected synthetic BES signal (blue), the noisy synthetic BES signal, generated by the detailed noise model (yellow) and the experimental signal (green) are featured in images A and B. Figure 3, Image A. shows a good agreement in the experimental and noisy synthetic signal features, overcoming the systematic discrepancy between the S and K of the experimental signals and their respective expected synthetic BES signals. This trend is enforced by the radial S profile featured in image B. showing a strong dampening of the S in the HESEL density signals in the near SOL, while the noisy and

experimental signals show a good agreement. Figure 4. shows a quantitative validation effort where filaments in thier respective signals were identified and their average waveform (image A.) and frequency computed (image B.). In addition to the data in Figure 3 purple featured the processes noisy synthetic BES signal, having been subjected to a 20 kHz lowpass Butterwoth filter, similarly as the experimental data. A good agreement was achieved between the processed synthetic BES signals and experimental signals, both in the averaged filament waveform as well as the radial filament frequency profile.

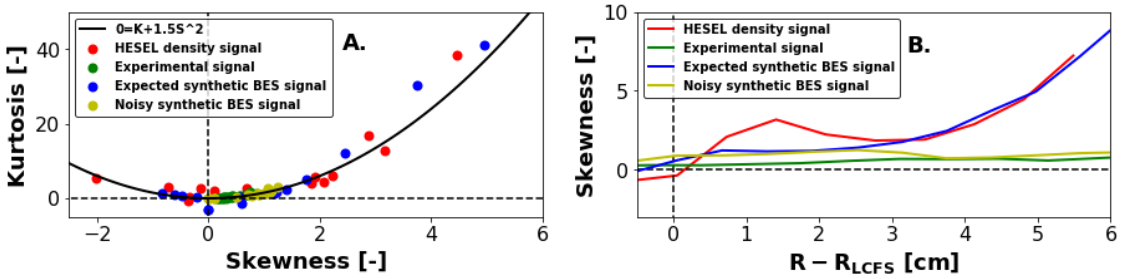

Figure 3: A. shows the skewness and kurtosis of various experimental and corresponding synthetic measurement channels. B. shows the radial skewness profile along the BES system for various synthetic and experimental measurement instances.

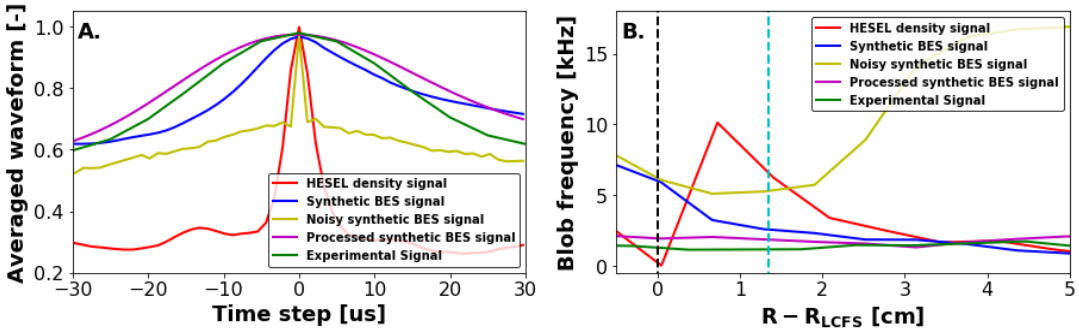

Figure 4: shows the averaged filament waveform (A) and the radial filament frequency profile for various synthetic and experimental measurement instances.

Summary A clear definition was given for synthetic BES diagnostics aimed at plasma fluctuation studies. A good qualitative and quantitative agreement was reached using a turbulence workflow coupled to synthetic BES diagnostics on ASDEX-Upgrade. Two different noise models were explored, showing the need for detailed noise modelling to correctly handle low photon count observation geometries.

Acknowledgement This work has been carried out within the framework of the EUROfusion Consortium and has received funding from the EuratomResearch and Training Programme 2014–2018 and 2019–2020 under Grant agreement No. 633053. The views and opinions expressed herein do not necessarily reflect those of the European Commission. G I Pokol and O. Asztalos acknowledge the support of the National Research, Development and InnovationOffice (NKFIH) Grant FK132134.

References:

[1] D.A. D'Ippolito et al., PoP. 18 (2011) 060501
[2] G.L. Falchetto et al., NF 54 (2014) 043018
[3] A.H. Nielsen et al., PPCF 59 (2017) 025012
[4] D. Guszejnov et al., RSI 83 (2012) 113501
[5] G. Birkenmeier et al., PPCF 56 (2014) 075019
[6] A.H. Nieslen et al., NF 59 (2019) 086059
[7] O. Asztalos et al., 45th EPS (2017) P4.109
[8] Hamamatsu R928 Manual
[9] D. Dunai et al., RSI 81 (2010) 103503